Multipath Performance of Adaptive Antennas with Multiple Interferers and Correlated Fadings

Tien D. Pham, *Member, IEEE,* and Keith G. Balmain, *Life Fellow, IEEE*

***Abstract*— This paper presents an approximate analytical cumulative distribution function of the output signal-to-noise-plus-interference ratio (SINR) of an adaptive antenna operating in multipath environments with multiple interferers and correlated fadings. Previously, approximate analytical results were only available for the case of one interferer and independent fadings between antenna branches, whereas in other cases Monte Carlo simulations had to be used with many limitations including excessive computer time and inaccurate results for small probability levels. The distribution, expressed in terms of the mean eigenvalues of the system, is accurate in most cases investigated even though it is based on an approximation to the characteristic function of the output SINR. As a result, a closed-form expression of bit error rate (BER) for coherent phase-shift keying (PSK) has been derived based on this approximation.**

***Index Terms*— Adaptive antennas, correlated fadings, multipath propagation.**

I. Introduction

WHILE ADAPTIVE antennas operating in nonmultipath environments have been subject to extensive research and widely used in military and satellite communications for interference suppression [1], [2], their ability to reduce both fading and cochannel interference in multipath environments has begun to gain interest as an attractive way to increase system capacity of mobile radio communications [3]–[6]. In the absence of interference, and with noise as the only undesired signal, an adaptive antenna performs the same task as a diversity antenna with maximal ratio combining, which is maximizing the signal-to-noise ratio (SNR). In the presence of strong interference, however, an adaptive antenna with the associated optimum combining has a superior performance compared with maximal ratio combining because the signal-to-noise-plus-interference ratio (SINR) is subject to optimization. The performance of an adaptive antenna, or optimum combiner, in the presence of interference and thermal noise was investigated by Winters [3], but the approximate analytical results are for the case of a single interferer only. For the case of multiple interferers, Monte Carlo simulations were used with limitations including excessive computer time and inaccurate results for small probability levels.

Manuscript received June 27, 1996; revised March 18, 1997.

T. D. Pham was with the Department of Electrical and Computer Engineering, University of Toronto, Toronto, Ont., M5S 3G4, Canada. He is now with the Wireless Research and Development Group, Mentor Graphics Corporation, San Jose, CA 95131-2314 USA.

K. G. Balmain is with the Department of Electrical and Computer Engineering, University of Toronto, Toronto, Ont., M5S 3G4, Canada.

Publisher Item Identifier S 0018-9545(99)01027-0.

Another problem needed to be addressed is the evaluation of adaptive antenna performance in the presence of correlated fadings, which are caused by either lack of independent propagation paths, compact designs of antennas, proximity effects of nearby disturbing objects [7], or a combination of these factors. In [8], Salz and Winters studied the effect of correlated fadings on adaptive antennas using Monte Carlo simulations, where branch correlations were due to narrow arrival beamwidth of the signals. In a more general scenario, unequal branch gains should also be considered. While the performance of maximal ratio combining in the presence of correlated fadings has been studied by Pierce and Stein [9] and analytical results obtained for arbitrary branch correlations and gains, a similar analysis is still needed for optimum combining.

In this paper, an approximate analytical cumulative distribution function (CDF) of the output SINR of adaptive antennas in the presence of multiple interferers and correlated flat fadings will be derived in order to address simultaneously the problems mentioned above. With the probability density function (PDF) known, the bit error rate (BER) of an optimum combiner can be obtained analytically for various modulation schemes. The results are general in several aspects including arbitrary branch correlations and branch gains for each of the desired and interfering signals, taking into account that these signals may have different propagation conditions and hence their source distributions at the receiving site may be different. Furthermore, as a special case of optimum combining, the CDF for maximal ratio combining with correlated fadings is the same as obtained previously [9].

II. CDF of the Output SINR of an Optimum Combiner

In the following derivation, unless otherwise stated, capital bold letters are reserved for matrices, small bold letters are for column vectors, the superscripts *, T, and H denote complex conjugate, transpose and Hermitian transpose, respectively.

A. Background

An adaptive array having M branches is shown in Fig. 1. The complex baseband signal received by the ith branch $x_i(t)$ is multiplied by a controllable weight w_i and the weighted signals are summed to form the output signal $y(t)$.

Consider the general situation of having one desired and L interfering signals transmitted. All signals are assumed to be narrowbanded and subject to flat Rayleigh fading at each antenna branch. Let $s_0(t)$ and $s_j(t)$ be the desired and jth

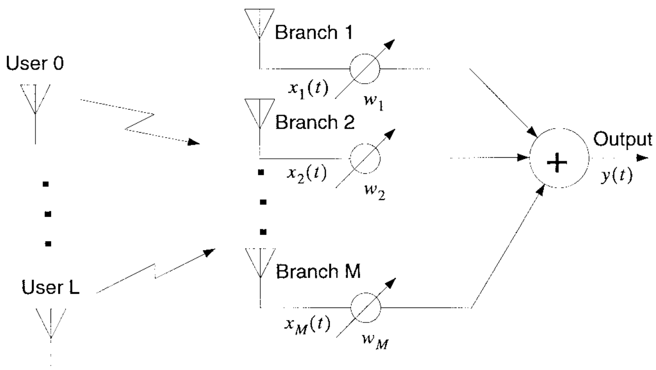

Fig. 1. An M-branch adaptive antenna with $(L+1)$ users.

interfering signals as they are transmitted, respectively, with the local average power

$$E[s_j(t)] = 1, \qquad 0 \le j \le L \tag{1}$$

where the expectation $e[\ ]$ is taken over a period much less than the reciprocal of the fading rate. Furthermore, let

$$\boldsymbol{u}_j = [u_{j1} \cdots u_{jM}]^1, \qquad 0 \le j \le L \tag{2}$$

be the complex propagation vector for the jth signal. Thus, u_{ji} is a complex Gaussian random variable that represents Rayleigh fading of the jth signal at the ith branch. Since the signals are transmitted independently, different signals received at a given branch are assumed to undergo independent fadings whereas signals received at different branches but originating from a single source are not necessarily independent because of mutual coupling and finite spacing between the branches. Mathematically, the received signals are assumed to have the following statistics:

$$\begin{aligned} \langle u_{ji} \rangle &= 0 \\ \langle u_{ji} u_{lk}^* \rangle &= 0, \qquad \text{for } 0 \le j, l \le L, 1 \le i, k \le M, j \ne l \end{aligned} \tag{3}$$

and

$$i = \langle \boldsymbol{u}_j \boldsymbol{u}_j^H \rangle = \begin{bmatrix} \langle u_{j1} u_{j1}^* \rangle & \cdots & \langle u_{j1} u_{jM}^* \rangle \\ & \cdots & \\ \langle u_{jM} u_{j1}^* \rangle & \cdots & \langle u_{jM} u_{jM}^* \rangle \end{bmatrix} \tag{4}$$

is the covariance matrix of the jth signal, where $\langle\ \rangle$ denotes average over Rayleigh fading.

The total signal received at the array consists of the desired signal, thermal noise, and interference and can be expressed in vector form as

$$\boldsymbol{x} = \sum_{j=0}^{L} \boldsymbol{x}_j + \boldsymbol{n} = \sum_{j=0}^{L} \boldsymbol{u}_j s_j + \boldsymbol{n} \tag{5}$$

where $\boldsymbol{x} = [x_1 \cdots x_M]^1$. $\boldsymbol{x}_j$ and $\boldsymbol{n}$ are the received jth signal and noise vectors, respectively, and are defined in the same manner.

The interference-plus-noise short-term covariance matrix is given by

$$\Phi = E\left[\left(\sum_{j=1}^{L} \boldsymbol{x}_j + \boldsymbol{n}\right)\left(\sum_{j=1}^{L} \boldsymbol{x}_j + \boldsymbol{n}\right)^H\right]. \tag{6}$$

If noise and interfering signals are uncorrelated in short term, it can be shown that

$$\Phi = \sigma^2 \boldsymbol{I} + \sum_{j=1}^{L} E[\boldsymbol{u}_j \boldsymbol{u}_j^H] \tag{7}$$

where $\boldsymbol{I}$ is the identity matrix and we have assumed that all branches have the same noise power $E[n_j n_j^*] = \sigma^2$. As the expected value in (7) is taken over a period much less than the reciprocal of the fading rate, the propagation vector $\boldsymbol{u}_j$ is assumed to be constant over this period and we have

$$\Phi = \sigma^2 \boldsymbol{I} + \sum_{j=1}^{L} \boldsymbol{u}_j \boldsymbol{u}_j^H. \tag{8}$$

With optimum combining, the output SINR [3] is given by

$$\gamma = \boldsymbol{u}_0^H \Phi^{-1} \boldsymbol{u}_0. \tag{9}$$

Note that γ is a random variable that varies at the fading rate and its CDF can be determined as shown in the next section.

B. Derivation of the CDF of Output SINR

Since the propagation vectors $\boldsymbol{u}_j, 0 \le j \le L$ are complex, it is most convenient to introduce the complex multivariate Gaussian density function of $\boldsymbol{u}_j$

$$p_j(\boldsymbol{u}_j) = \frac{1}{\pi^M |\boldsymbol{R}_i|} \exp(-\boldsymbol{u}_j^H \boldsymbol{R}_j^{-1} \boldsymbol{u}_j), \qquad 0 \le j \le L \tag{10}$$

where $|\ |$ denotes determinant [10, p. 507]. Note that this definition is possible because $\boldsymbol{R}_j$ is Hermitian. Since all signals are assumed to have independent fadings, the joint density function of $\boldsymbol{u}_1, \cdots, \boldsymbol{u}_L$ is given by

$$p_u(\boldsymbol{u}_0, \cdots, \boldsymbol{u}_L) = \prod_{j=0}^{L} p_j(\boldsymbol{u}_j). \tag{11}$$

The PDF of the output SINR can be found by first determining the characteristic function of through the Laplace transform

$$\Psi(z) = \int_0^\infty p(\gamma) \exp(-z\gamma)\, d\gamma. \tag{12}$$

Note that $\gamma \ge 0$, i.e., $p(\gamma) = 0$ for $\gamma < 0$, so

$$\begin{aligned} \Psi(z) &= \langle \exp(-z\gamma) \rangle \\ &= \int_{-\infty}^{\infty} \cdots \int_{-\infty}^{\infty} p_u(\boldsymbol{u}_0, \cdots, \boldsymbol{u}_L) \\ &\quad \cdot \exp(-z \boldsymbol{u}_0^H \Phi^{-1} \boldsymbol{u}_0)\, d\boldsymbol{u}_0 \cdots d\boldsymbol{u}_L \qquad (13) \\ &= \int_{-\infty}^{\infty} \cdots \int_{-\infty}^{\infty} p_1(\boldsymbol{u}_1), \cdots, p_L(\boldsymbol{u}_L)\, d\boldsymbol{u}_1 \cdots d\boldsymbol{u}_L \\ &\quad \cdots G(z, \boldsymbol{u}_1, \cdots, \boldsymbol{u}_L) \qquad (14) \end{aligned}$$

where

$$\begin{aligned} G(z, \boldsymbol{u}_1, \cdots, \boldsymbol{u}_L) &= \int_{-\infty}^{\infty} p_0(\boldsymbol{u}_0)\ \exp(-z\boldsymbol{u}_0^H \Phi^{-1}\boldsymbol{u}_0)\ d\boldsymbol{u}_0 \\ &= \frac{1}{\pi^M |\boldsymbol{R}_0|} \int_{-\infty}^{\infty} \exp[-\boldsymbol{u}_0^H(\boldsymbol{R}_0^{-1} + z\Phi^{-1})\boldsymbol{u}_0]\ d\boldsymbol{u}_0 \\ &= \frac{1}{\pi^M |\boldsymbol{R}_0|} \frac{\pi^M}{|\boldsymbol{R}_0^{-1} + z\Phi^{-1}|} \\ &= \frac{1}{|\boldsymbol{I} + z\boldsymbol{R}_0\Phi^{-1}|}. \end{aligned} \tag{15}$$

The exact evaluation of the integral in (14) is shown in Appendix A with the matrix $\boldsymbol{R}_0^{-1} + z\Phi^{-1}$ being Hermitian. $G(z, \boldsymbol{u}_1, \cdots, \boldsymbol{u}_L)$ can be rewritten as follows:

$$G(z, \boldsymbol{u}_1, \cdots, \boldsymbol{u}_L) = G(z, \lambda_1, \cdots, \lambda_M) = \frac{1}{\prod_{i=1}^{M} \left(1 + \frac{z}{\lambda_i}\right)} \tag{16}$$

where $\lambda_1, \cdots, \lambda_M$ are the eigenvalues of $(\boldsymbol{R}_0\Phi^{-1})^{-1} = \Phi\boldsymbol{R}_0^{-1}$. They are, equivalently, solutions to the generalized eigenvalue problem

$$\Phi\boldsymbol{v} = \lambda\boldsymbol{R}_0\boldsymbol{v}. \tag{17}$$

The characteristic function given in (13) is just the expectation of $G(z, \lambda_1, \cdots, \lambda_L)$ with respect to $\lambda_1, \cdots, \lambda_M$

$$\Psi(z) = \langle G(z, \lambda_1, \cdots, \lambda_M)\rangle \tag{18}$$

which is extremely difficult, if at all possible, to evaluate exactly. An estimate of $\Psi(z)$ can be made by using the usual technique of expanding $G(z, \lambda_1, \cdots, \lambda_L)$ in a Taylor series from which $\Psi(z)$ can be expressed in terms of mean, covariance and higher moments of $\lambda_1, \cdots, \lambda_M$ [11, p. 156]. It turns out that the first-order approximation

$$G(z, \lambda_1, \cdots, \lambda_M)\rangle \cong G(z, \langle\lambda_1\rangle, \cdots, \langle\lambda_M\rangle) \tag{19}$$

yields accurate results in most cases. Thus

$$\Psi(z) \cong \prod_{i=1}^{M} \left(\frac{1}{1 + \frac{z}{\langle z_i\rangle}}\right) = \prod_{i=1}^{M} \left(\frac{\langle\lambda_1\rangle}{z + \langle\lambda_i\rangle}\right). \tag{20}$$

The PDF of the output SINR can now be determined by an inverse Laplace transform of $\Psi(z)$. By using a partial fraction expansion [12, p. 674], $\Psi(z)$ can be written as a sum of simple fractions whose inverse Laplace transforms are known. The M mean eigenvalues appearing in (20) are all real and positive due to the positive definite and Hermitian nature of Φ and $\boldsymbol{R}_0$. As will be discussed later, there are $N, N < M$ mean eigenvalues of multiplicities one and mean eigenvalue of multiplicity $(M - N)$ in the most general case of interest, i.e., $\langle\lambda_1\rangle \neq \cdots \neq \langle\lambda_N\rangle \neq \langle\lambda_{N+1}\rangle = \cdots = \langle\lambda_M\rangle$, hence, (20) can be written in the form

$$\Psi(z) = \sum_{i=1}^{N} \frac{B_i}{z + \langle\lambda_i\rangle} + \sum_{i=1}^{M-N} \frac{C_i}{(z + \langle\lambda_M\rangle)^i} \tag{21}$$

where

$$B_i = \lim_{z \to -\langle\lambda_i\rangle} \{\Psi(z)(z + \langle\lambda_i\rangle)\} \tag{22}$$

and

$$\begin{aligned} C_i = \frac{1}{(M - N - i)!} \lim_{z \to -\langle\lambda_M\rangle} \left(\frac{d}{dz}\right)^{M-N-1} \\ \cdot \{\Psi(z)(z + \langle\lambda_M\rangle)^i\}. \end{aligned} \tag{23}$$

From the table of inverse Laplace transforms, the PDF is found to be

$$\begin{aligned} p(\gamma) &= \mathcal{L}^{-1}\{\Psi(z)\} \\ &= \sum_{i=1}^{N} B_i\ \exp(-\langle\lambda_i\rangle\gamma) \\ &\quad + \sum_{i=1}^{M-N} C_i \frac{\gamma^{i-1}}{(i-1)!} \exp(-\langle\lambda_M\rangle\gamma). \end{aligned} \tag{24}$$

Hence, the CDF of the output SINR is

$$\begin{aligned} P(\gamma) &= \int_0^{\gamma} p(\xi)\ d\xi \\ &= \sum_{i=1}^{N} \frac{B_i}{\langle\lambda_i\rangle} [1 - \exp(-\langle\lambda_i\rangle\gamma] + \sum_{i=1}^{M-N} \frac{C_i}{\langle\lambda_M\rangle^i} \\ &\quad \cdot \left[1 - \sum_{k=}^{i-1} \frac{\gamma^k \langle\lambda_M\rangle^k}{k!} (\exp(-\langle\lambda_M\rangle\gamma))\right]. \end{aligned} \tag{25}$$

As a special case of (20), where all mean eigenvalues are distinct $(N = M)$

$$\Psi(z) = \sum_{i=1}^{M} \frac{B_i}{z + \langle\lambda_i\rangle} \tag{26}$$

$$\begin{aligned} B_i &= \lim_{z \to -\langle\lambda_i\rangle}; \{\Psi(z)(z + \langle\lambda_i\rangle)\} \\ &= \prod_{k=1, k\neq i}^{M} \left(\frac{\langle\lambda_k\rangle}{\langle\lambda_k\rangle - \langle\lambda_i\rangle}\right) \end{aligned} \tag{27}$$

$$p(\gamma) = \sum_{i=1}^{M} B_i\ \exp(-\langle\lambda_i\rangle\gamma) \tag{28}$$

$$P(\gamma) = \sum_{i=1}^{M} \frac{B_i}{\langle\lambda_i\rangle} [1 - \exp(-\langle\lambda_i\rangle\gamma)]. \tag{29}$$

C. Eigenvalue Analysis

The CDF of γ given by (25), (22), and (23) is general for optimum combining with M correlated branches and L interferers. The whole distribution is specified in terms of the mean eigenvalues of (17). Only in simple cases are analytical solutions for the eigenvalues known and hence their means determined, whereas in other cases we have to resort to Monte Carlo techniques to determine these values numerically.

1) Thermal Noise—No Interferer—Correlated Branches: In the absence of interference, the undesired signals consist of only thermal noise, and are thus uncorrelated between branches, i.e. $\Phi = \sigma^2 \boldsymbol{I}$. The generalized eigenvalue problem (17) is reduced to

$$\sigma^2 \boldsymbol{I}\boldsymbol{v} = \lambda \boldsymbol{R}_0 \boldsymbol{v} \tag{30}$$

which is a deterministic problem where $\langle\lambda_i\rangle = \lambda_i, 1 \le i \le M$ can be found by any standard method. Since there is no interference, the adaptive antenna merely works as a diversity antenna with maximal ratio combining, which has been studied by Pierce and Stein previously [9].

2) Thermal Noise—One Interferer—Uncorrelated Branches: Suppose the antenna elements have the same gain and are separated by sufficiently large element spacings such that the branch signals are uncorrelated. Then the covariance matrices of the signals can be written as

$$\boldsymbol{R}_j = P_j \boldsymbol{I}, \qquad 0 \le j \le L \tag{31}$$

where

$$P_j = \langle u_{ji} u_{ji}^* \rangle, \qquad 1 \le i \le M \tag{32}$$

is the average received jth signal power at the ith branch. In the presence of thermal noise and one interferer, we have

$$\Phi = \sigma^2 \boldsymbol{I} + \Phi_u \tag{33}$$

where $\Phi_u = \boldsymbol{u}_1 \boldsymbol{u}_1^H$ is the interference short term covariance matrix. Thus, the generalized eigenvalue problem (17) becomes

$$(\sigma^2 \boldsymbol{I} + \Phi_u)\boldsymbol{v} = \lambda P_0 \boldsymbol{v} \tag{34}$$

or

$$\Phi_u \boldsymbol{v} = (\lambda P_0 - \sigma^2)\boldsymbol{v}. \tag{35}$$

From here, it can be seen that

$$\alpha_i = \lambda_i P_0 - \sigma^2, \qquad 1 \le i \le M \tag{36}$$

where α_i are the eigenvalues of Φ_u, which is an $M \times M$ matrix of rank 1. The α_i are given by

$$\alpha_i = \begin{cases} 0, & \text{for } 1 \le i \le M-1 \\ \boldsymbol{u}_1^H \boldsymbol{u}_1, & \text{for } i = M \end{cases} \tag{37}$$

thus their means are given by

$$\langle\alpha_i\rangle = \begin{cases} 0, & \text{for } 1 \le i \le M-1 \\ MP_1, & \text{for } i = M. \end{cases} \tag{38}$$

It follows from (36) and (38) that

$$\langle\lambda_i\rangle = \begin{cases} \sigma^2/P_0, & \text{for } 1 \le i \le M-1 \\ (MP_1 + \sigma^2)/P_0, & \text{for } i = M. \end{cases} \tag{39}$$

Normally, the jth signal-to-noise ratio defined as

$$\Gamma_j = \frac{P_j}{\sigma^2}, \qquad 0 \le j \le L \tag{40}$$

is known, so the mean eigenvalues can be expressed as

$$\langle\lambda_i\rangle = \begin{cases} 1/\Gamma_0, & \text{for } 1 \le i \le M-1 \\ (M\Gamma_1 + 1)/\Gamma_0, & \text{for } i = M. \end{cases} \tag{41}$$

TABLE I
INTRINSIC MEAN EIGENVALUES, $a_i = \langle\alpha_i\rangle/P_1$

	$L = 1$	2	3	4	5
$M = 1$	1.00	2.00	3.00	4.00	5.00
2	0.00	0.50	1.12	1.81	2.54
	2.00	3.50	4.88	6.19	7.46
3	0.00	0.00	0.33	0.79	1.32
	0.00	1.12	2.15	3.16	4.16
	3.00	4.88	6.52	8.05	9.52
4	0.00	0.00	0.00	0.25	0.61
	0.00	0.00	0.79	1.57	2.37
	0.00	1.81	3.16	4.41	5.63
	4.00	6.19	8.05	9.77	11.39
5	0.00	0.00	0.00	0.00	0.20
	0.00	0.00	0.00	0.61	1.24
	0.00	0.00	1.32	2.37	3.39
	0.00	2.54	4.16	5.63	7.01
	5.00	7.46	9.52	11.39	13.16

We see that the smallest mean eigenvalue, which has a multiplicity of $(M-1)$, is proportional to the noise power while the largest one is proportional to the total interference plus noise power. Mathematically, the corresponding eigenvectors are said to span the noise and interference-plus-noise subspaces, respectively [13, p. 377]. With the mean eigenvalues given in (41), the CDF of the output SINR given by (25) where $N = 1$ is fully specified. Essentially the same results were obtained by Bogachev and Kiselev [14] using another technique, but their results were given in integral form which seems less manageable than (25). The results of a four-branch adaptive antenna with one interferer are shown in the next section as a special case of the multiple-interferer case.

3) Thermal Noise—Multiple Interferers—Uncorrelated Branches: This case is similar to case 2 with the interference short term covariance matrix given by

$$\Phi_u = \sum_{j=1}^{L} \boldsymbol{u}_j \boldsymbol{u}_j^H \tag{42}$$

whose eigenvalues are no longer as simple as given in (37). An analytical expression for α_i is at best intricate in some cases and difficult if not impossible to find in others. By using a Monte Carlo technique, however, we can determine $\langle\alpha_i\rangle$ and hence $\langle\lambda_i\rangle$ numerically. We still assume all branches have the same average gain [(32)], and furthermore, we assume all interfering signals have the same strength, i.e., $P_j = P_1, 1 \le j \le L$. The intrinsic mean eigenvalues defined as $a_i = \langle\alpha_i\rangle/P_1$ are obtained from 10 000 sample Monte Carlo averaging and are shown in Table I for several values of M and L.

The mean eigenvalues for each (M, L) pair in the table are arranged in ascending order and their sum is seen to be equal to the total interference power incident upon the array, which is $M \times L$. Since Φ_u is an $M \times M$ matrix of rank L, we see that only L eigenvalues and hence their means are nonzero for each (M, L) pair. It is straightforward to show that the zero eigenvalues give rise to an infinite output SINR if there is no thermal noise, which explains why an branch adaptive antenna can null up to $L = M - 1$ interferers. Hence, it can be expected that if the interference is the dominant

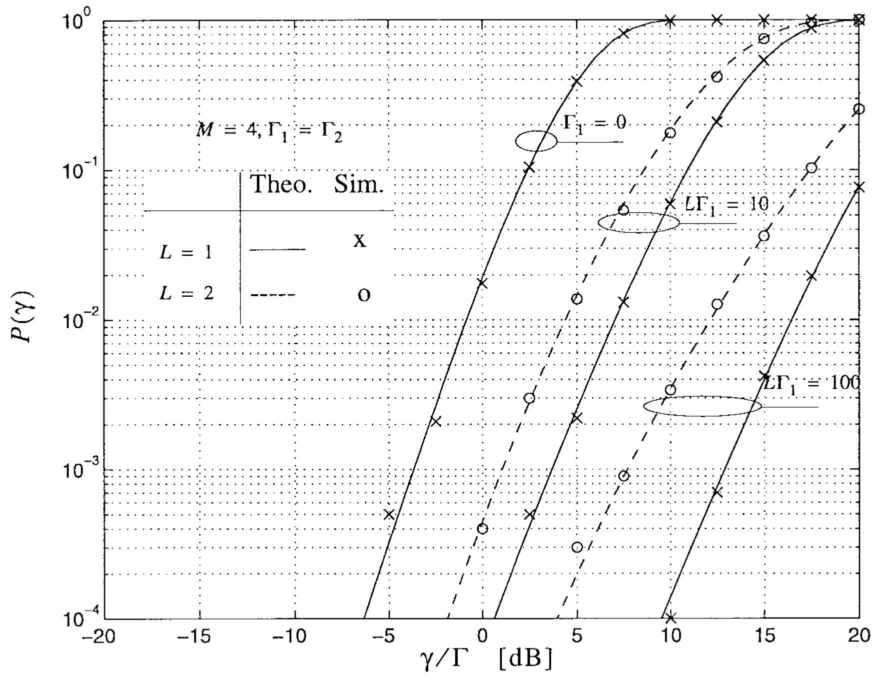

Fig. 2. The CDF of the output SINR of an adaptive antenna with four uncorrelated branches and several interferers.

source of undesired signals, the output SINR of the array will be significantly improved over the branch SINR. It is also interesting to note that the nonzero eigenvalues of the M branch and L interferer case are the same as those in the L branch and M interferer case. This can be proven to be valid for any values of M and L provided: 1) the branches are uncorrelated; 2) all branches have same average gain; and 3) all interferers have same average power.

It follows from (36) that

$$\langle \lambda_i \rangle = \frac{\langle \alpha_i \rangle + \sigma^2}{P_0} = \frac{a_i P_1 + \sigma^2}{P_0} = \frac{a_i \Gamma_1 + 1}{\Gamma_0}, \quad 1 \le i \le M. \tag{43}$$

From Table I, (25), and (43), the CDF of the output SINR can be determined for arbitrary levels of input INR and SNR. An extended table for larger values of M and L can be worked out if one needs to evaluate the performance of larger arrays.

As an example, we calculate the mean eigenvalues of a four-branch array with several equal strength interferers and plot the CDF for each case. Let the desired and total interfering signal powers be 10 dB over the noise level, i.e., $\Gamma_0 = L\Gamma_1 = 10$. The mean eigenvalues according to Table I and (43) are:

1) $M = 4, L = 1$: $\langle \lambda_1 \rangle = \langle \lambda_2 \rangle = \langle \lambda_3 \rangle = 0.1, \langle \lambda_4 \rangle = 4.1$;
2) $M = 4, L = 2$: $\langle \lambda_1 \rangle = \langle \lambda_2 \rangle = 0.1, \langle \lambda_3 \rangle = 1.005, \langle \lambda_4 \rangle = 3.195$.

Fig. 1 shows the CDF of γ versus γ/Γ, where

$$\Gamma = \frac{P_0}{\sum_{i=1}^{L} P_j + \sigma^2} = \frac{\Gamma_0}{\sum_{i=1}^{L} \Gamma_j + 1} \tag{44}$$

is the mean branch SINR. The analytical curves are seen to agree closely with results from 10 000 sample Monte Carlo simulations. At low-probability levels, the simulation results tend to deviate randomly around the analytical curves due to the limited number of samples used in the simulations. Analytical and simulation results for other INR levels are also shown in Fig. 2. Due to the normalization of the abscissa, the branch undesired signal power appears to be constant, so we see that as the interference power becomes a dominant part of the undesired signal power, the performance of the array improves. For $\Gamma_1 = 0$, i.e., there is no interference, the performance is the same as that of a maximal ratio combiner. For $L\Gamma_1 = 100$, the performance of the array is improved by 17 and 13 dB for $L = 1$ and $L = 2$, respectively, at 1% probability level. As the number of interferers increases, the sum of the interfering signals becomes decorrelated between branches and behaves more like noise. Therefore, it can be expected that for $L \to \infty$, the CDF curves should approach those of the maximal ratio combiner.

4) Thermal Noise—Multiple Interferers—Correlated Branches: This is the most general case in the sense that there can be any number of interferers incident upon an array with arbitrary correlations between the branches and arbitrary average powers in each. Since the desired and interfering signals may have different propagation conditions and hence their angular source distributions at the receiving site can all be different, their covariance matrices $\boldsymbol{R}_j, 0 \le j \le L$ are most generally not the same. It is not uncommon, however, that the propagation conditions for one signal are equally favorable to others, such as in a crowded indoor environment: then it can be shown that their covariance matrices are either the same or different just by proportionality constants.

The eigenvalues $\lambda_i, 1 \le i \le M$, to be found are solutions to the generalized eigenvalue problem (17), where Φ is still given by (33) and (42), but $\boldsymbol{R}_0$ is no longer proportional to an identity

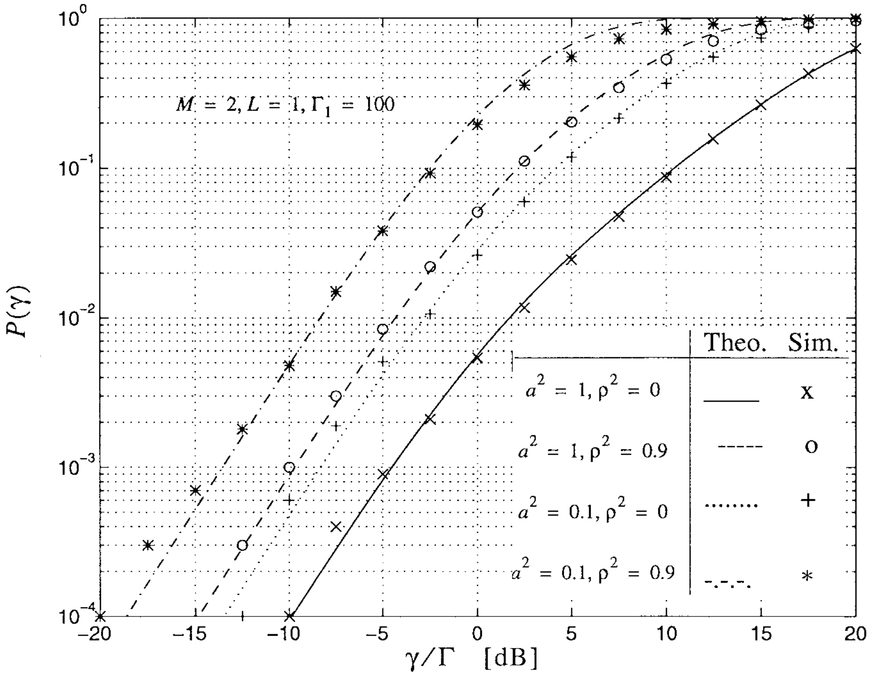

Fig. 3. The CDF of the output SINR of an adaptive antenna with two correlated branches and one interferer.

matrix as in (31). In order to find $\langle\lambda_i\rangle$ a Monte Carlo technique is again used, where the random vectors $\boldsymbol{u}_j, 0 \leq j \leq L$ are generated according to the covariance matrices $\boldsymbol{R}_j$ (see Appendix B). Unfortunately, there is no simple relationship between the mean eigenvalues $\langle\lambda_i\rangle$ and $\langle\alpha_i\rangle$ as in (43) so $\langle\lambda_i\rangle$ have to be determined by a Monte Carlo technique for particular values of INR's.

As an example, we calculate the mean eigenvalues for a two branch array with one interferer. In order to investigate the effects of unequal branch gains and branch correlation, we let the desired and interfering signals have the following covariance matrices:

$$\boldsymbol{R}_0 = \boldsymbol{R}_1 = \begin{bmatrix} 1 & a\rho \\ a\rho & a^2 \end{bmatrix} \tag{45}$$

where ρ is the branch correlation and a^2 is the gain ratio between the second and the first branches. Furthermore, let the desired and interfering signal powers be 20 dB over the noise level, i.e., $\Gamma_0 = \Gamma_1 = 100$; then we have:

1) $\rho^2 = 0, a^2 = 1$: $\langle\lambda_1\rangle = 0.01, \langle\lambda_2\rangle = 2.01$;
2) $\rho^2 = 0.9, a^2 = 1$: $\langle\lambda_1\rangle = 0.09, \langle\lambda_2\rangle = 2.11$;
3) $\rho^2 = 0, a^2 = 0.1$: $\langle\lambda_1\rangle = 0.05, \langle\lambda_2\rangle = 2.05$;
4) $\rho^2 = 0.9, a^2 = 0.1$: $\langle\lambda_1\rangle = 0.40, \langle\lambda_2\rangle = 2.70$.

Fig. 3 shows the CDF of γ versus γ/Γ for the above cases. The analytical results for the first three cases are seen to agree closely with results from 10 000 sample Monte Carlo simulations except at low-probability levels where the simulation results are not very accurate due the limited number of samples. For the last case, however, there are small deviations between analytical and simulation results for probabilities larger than 0.1. Since simulation results can be expected to be accurate at such high-probability levels, we conclude that it is the analytical results that are inaccurate in this case, recalling that the CDF of γ is only based on a first-order approximation of its characteristic function. The deviation is, however, not very large and we are usually interested in small probability levels, which are analytically accurate. The difference in the output SINR's of cases 1) and 2) is the performance degradation due to branch correlation. At the 1% probability level, the degradation is seen to be 6 dB. Similarly, from case 3), the degradation due to unequal branch gains is 4.5 dB, whereas a degradation of approximately 10 dB is seen in case 4) as a result of the combined effects of branch correlation and unequal branch gains.

D. Convergence of Analytical and Numerical CDF's

Even though the derived analytical CDF is based on a first-order approximation of $\langle G(z, \lambda_1, \cdots, \lambda_M)\rangle$, which is given by (19), the results are accurate in all but one case investigated in the previous section. The reason why this first-order approximation works is because G is a well-behaved smooth function of λ_i as is evident from (16), and, therefore, the high-order terms of the approximation can be expected to be very small.

In Section C, good agreement between analytical and numerical results by Monte Carlo simulations has been observed for probability levels as small as 10^{-4}. By increasing the number of samples in the simulations, the results can be shown to agree at even smaller probability levels. Consider again the four-branch array and several equal strength interferers with $L\Gamma_1 = 100$. Fig. 4 shows the numerical results of 100 000 and 1 000 000 sample simulations, which evidently converge toward the analytical CDF for all probability levels down to 10^{-6}. Similarly, for the case of the two-branch array

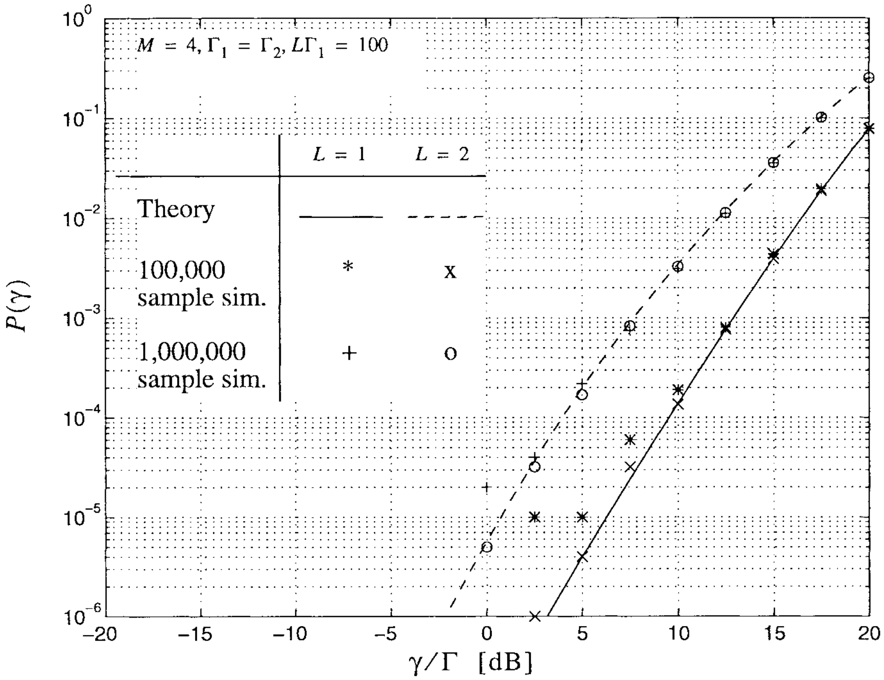

Fig. 4. Same as in Fig. 3 with $L\Gamma_1 = 100$ and the number of samples in the simulations increased to 100 000 and 1 000 000.

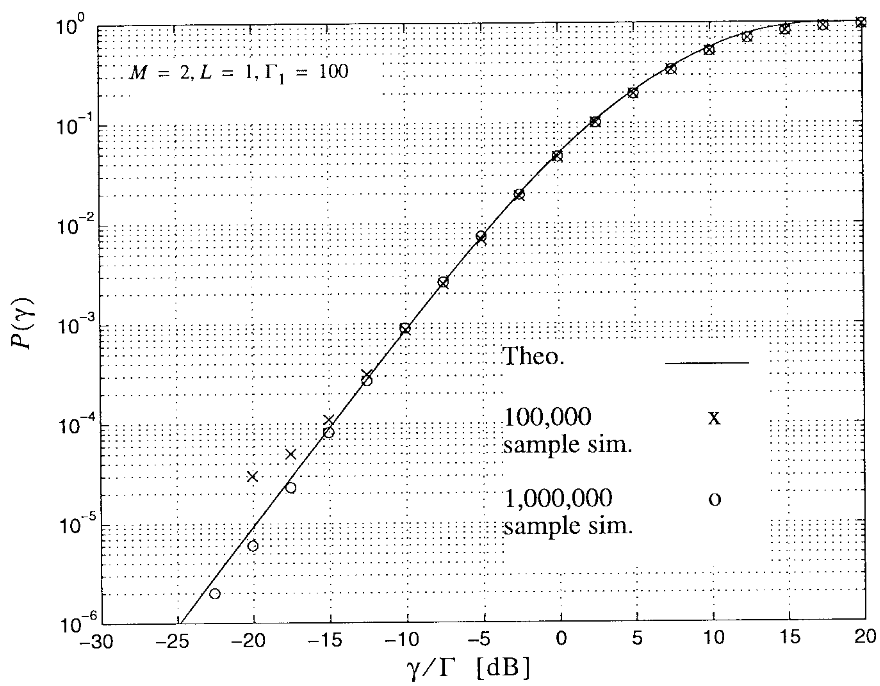

Fig. 5. Same as in Fig. 3 with $a^2 = 1, \rho^2 = 0.9$, and the number of samples in the simulations increased to 100 000 and 1 000 000.

having correlation coefficient $\rho^2 = 0.9$ and one interferer with $\Gamma_1 = 100$, Fig. 5 shows the convergence of the numerical results as the number of samples increases from 100 000 to 1 000 000.

As discussed under point 4) in Section C, the mean eigenvalues must be determined by a Monte Carlo technique for the case of correlated branches. While one may think that this defeats the purpose of deriving the analytical CDF, the CDF expressed in terms of the mean eigenvalues still offers a significant advantage over full Monte Carlo simulation because determining the mean eigenvalues requires fewer samples by far than finding the numerical CDF directly. Once the mean eigenvalues have been found, the distribution is fully known, i.e., the probability at any output level can be found.

Consider for example an array having five correlated branches and three equal strength interferers with $L\Gamma_1 = 100$.

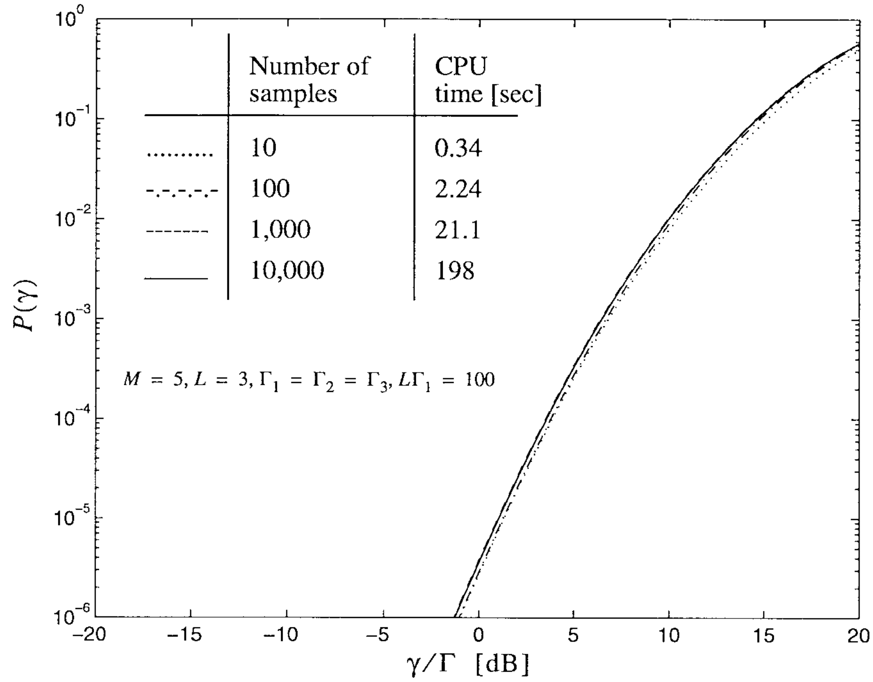

Fig. 6. The analytical CDF's of the output SINR of an adaptive antenna with five correlated branches and three interferers. The CDF's are based on mean eigenvalues calculated by Monte Carlo technique with different numbers of samples.

TABLE II
MEAN EIGENVALUES OF AN ADAPTIVE ANTENNA WITH FIVE CORRELATED BRANCHES AND THREE INTERFERERS, CALCULATED WITH DIFFERENT SAMPLE SIZES

	10 samples	100 sample	1,000 samples	10,000 samples
$\langle\lambda_1\rangle$	1.13×10^{-2}	1.32×10^{-2}	1.39×10^{-2}	1.39×10^{-2}
$\langle\lambda_2\rangle$	3.16×10^{-2}	3.33×10^{-2}	3.39×10^{-2}	3.34×10^{-2}
$\langle\lambda_3\rangle$	4.36×10^{-1}	4.13×10^{-1}	4.72×10^{-1}	4.63×10^{-1}
$\langle\lambda_4\rangle$	1.31	1.32	1.41	1.41
$\langle\lambda_5\rangle$	3.33	3.13	3.23	3.19

Assume that the desired and interfering signals have the following covariance matrix:

$$\boldsymbol{R}_0 = \boldsymbol{R}_1 = \begin{bmatrix} 1 & 0.6 & 0.3 & 0.3 & 0.6 \\ 0.6 & 1 & 0.6 & 0.3 & 0.3 \\ 0.3 & 0.6 & 1 & 0.6 & 0.3 \\ 0.3 & 0.3 & 0.6 & 1 & 0.6 \\ 0.6 & 0.3 & 0.3 & 0.6 & 1 \end{bmatrix}. \tag{46}$$

The mean eigenvalues calculated by the Monte Carlo technique with different numbers of samples are listed in Table II, which shows small differences between calculations, especially for those cases with the highest numbers of samples. The analytical CDF's based on these sets of mean eigenvalues are shown in Fig. 6. It is evident that the CDF's converge quickly as the number of samples increases. For 1000 and 10 000 samples, the CDF's are almost indistinguishable. It is worth noting that even when the number of samples is as small as ten, the approximate CDF is less than 0.5 dB from the converged CDF at all probability levels. For comparison, numerical CDF's obtained from Monte Carlo simulations are shown in Fig. 7 with the converged analytical CDF. Only the CDF with 1 000 000 samples is seen to match closely with the analytical CDF at all probablity levels shown. The central processing unit (CPU) time for the 1 000 000 sample simulation is 19 350 s, which is approximately 1000 times longer than that of 1000 sample calculation of the mean eigenvalues. If the numerical CDF is to be determined at probability levels lower than 10^{-6}, even more samples will be needed. Because of limitations in computer memory and CPU time, the Monte Carlo approach becomes impossible below a certain probability level, leaving the analytical CDF as the only known method to determine the SINR performance of an adaptive antenna with correlated branches at extremely low-probability levels.

E. BER Performance for Optimum Combining

In digital mobile communications, the average BER for coherent detection of phase-shift keying (PSK) signals is given by

$$\text{BER} = \tfrac{1}{2} \int_0^\infty p(\gamma)\, \text{erfc}(\sqrt{\gamma})\, d\gamma \tag{47}$$

where $p(\gamma)$ is the PDF of the output SINR.

Substituting (24) into (47), we have the BER performance for optimum combining with multiple interferers and correlated fadings

$$\begin{aligned} \text{BER} = \frac{1}{2} \int_0^\infty & \left(\sum_{i=1}^{N} B_i \exp(-\langle\lambda_i\rangle\gamma) \right. \\ & \left. + \sum_{i=1}^{M-N} C_i \frac{\gamma^{i-1}}{(i-1)!} \exp(-\langle\lambda_M\rangle\gamma) \right) \\ & \cdot \text{erfc}(\sqrt{\gamma})\, d\gamma. \end{aligned} \tag{48}$$

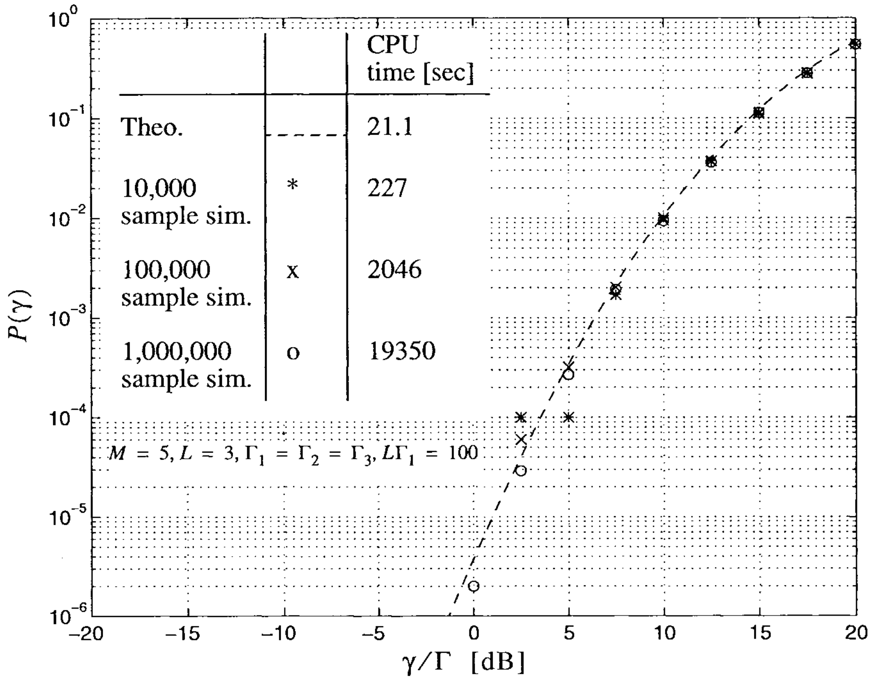

Fig. 7. The CDF of the output SINR of an adaptive antenna with five correlated branches and three interferers.

In order to evaluate (48), we need the following general integral formula [15]:

$$\frac{1}{2(K-1)} \int_0^\infty x^{K-1} \exp(-ax) \operatorname{erfc}(\sqrt{bx})\, dx \cdot \left(\frac{\sqrt{1+a/b}-1}{2a\sqrt{1+a/b}}\right)^K \sum_{k=0}^{K-1} \binom{K-1+k}{k} \cdot \left(\frac{\sqrt{1+a/b}+1}{2\sqrt{1+a/b}}\right)^k \tag{49}$$

where $\binom{K-1+k}{k} = ((K-1+k)!/k!(K-1)!)$ are binomial coefficients and $a > 0$.

From (48) and (49), we get

$$\mathrm{BER} = \sum_{i=1}^{N} B_i \left(\frac{\sqrt{1+\langle\lambda_i}-1}{2\langle\lambda_i\rangle\sqrt{1+\langle\lambda_i\rangle}}\right) + \sum_{i=1}^{M-N} C_i \left(\frac{\sqrt{1+\langle\lambda_i\rangle}-1}{2\langle\lambda_i\rangle\sqrt{1+\langle\lambda_i\rangle}}\right)^i \cdot \sum_{k=0}^{i-1} \binom{i-1+k}{k} \left(\frac{\sqrt{1+\langle\lambda_i\rangle}-1}{2\sqrt{1+\langle\lambda_i\rangle}}\right)^k \tag{50}$$

where B_i and C_i are given by (22) and (23), respectively. For the simple case of all distinct mean eigenvalues $(N = M)$, we have

$$\mathrm{BER} = \sum_{i=1}^{M} B_i \left(\frac{\sqrt{1+\langle\lambda_i\rangle}-1}{2\langle\lambda_i\rangle\sqrt{1+\langle\lambda_i\rangle}}\right) \tag{51}$$

where B_i is given by (27).

The BER versus mean branch SINR of adaptive antennas with several uncorrelated branches and two equal strength interferers is shown in Fig. 8. Note that the mean eigenvalues in (50) or (51) can be expressed in terms of Γ_1 and Γ as

$$\langle\lambda_i\rangle = \frac{a_i\Gamma_1 + 1}{\Gamma(L\Gamma_1+1)} \tag{52}$$

which follows directly from (43) and (44). These analytical results agree closely with results from 100 000 sample Monte Carlo simulations by Winters [3].

Similarly, for the case of arbitrary branch correlations and gains, one can determine the mean eigenvalues b_i of (17) for $\Gamma_0 = \Gamma_1$. The mean eigenvalues for any values of Γ_0 are

$$\langle\lambda_i\rangle = \frac{b_i\Gamma_1}{\Gamma_0} = \frac{b_i\Gamma_i}{\Gamma\left(\sum_{i=1}^{L}\Gamma_j + 1\right)} \tag{53}$$

assuming that all Γ_j are kept unchanged.

III. Conclusions

In this paper, an approximate analytical CDF of the output SINR of an adaptive antenna with correlated branches and multiple interferers in flat Rayleigh fading environments has been derived. Even though the distribution is based on an approximation to the characteristic function of the output SINR, it is accurate in all but one case investigated, namely, at high-probability levels when there are high branch correlations and large differences between branch powers.

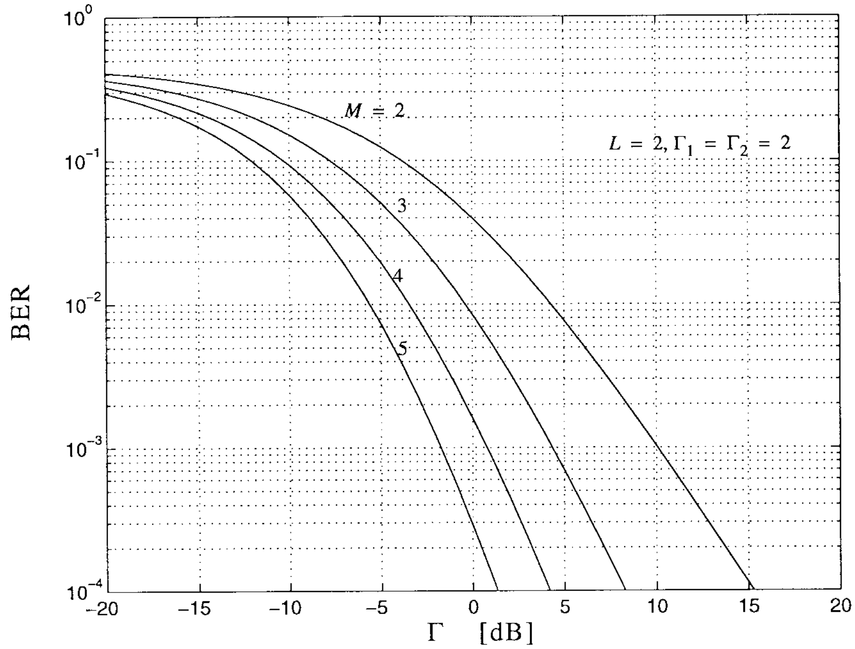

Fig. 8. The BER versus the mean branch SINR for adaptive antennas with several uncorrelated branches and two equal-strength interferers.

In the case of uncorrelated branches, the intrinsic mean eigenvalues for systems with several branches and equal-strength interferers have been tabulated. With this table, the mean eigenvalues for systems with arbitrary SNR and INR can be determined. Thus, the distribution offers a quick and accurate way to evaluate the performance of an adaptive antenna in multipath environments, especially at low-probability levels where results by Monte Carlo simulations are either unreliable or impractical because of limitations in computer time or memory.

In the case of correlated branches, the mean eigenvalues have to be determined numerically for particular values of INR's by a Monte Carlo technique. Nevertheless, the CDF expressed in terms of these mean eigenvalues still offers significant advantages over full Monte Carlo simulations because determining the mean eigenvalues requires fewer samples by far than finding the CDF directly. Furthermore, once the mean eigenvalues have been found, the distribution is fully known, i.e., the probability at any output level can be determined accurately.

As a result, a closed-form expression of BER for coherent PSK has been derived based on the above approximation. With the CDF available in terms of elementary functions, closed-form expressions of BER for many other digital modulations can be derived.

The CDF thus found should provide a powerful analytical tool for evaluation of adaptive antenna performance in multipath environments. With multiple interferers taken into account, the result is expected to be valuable in designing multiple-user radio systems where optimum combining is implemented to enhance interference tolerance and increase capacity [4]. With branch correlation and unequal branch gains considered, we can realistically estimate the performance of compact adaptive antennas, where design constraints and proximity effects of nearby disturbing objects often make the assumption of independent and equal-gain branches invalid [7].

Appendix A

Let

$$\boldsymbol{x} = \boldsymbol{u}_r + j\boldsymbol{u}_i, \qquad \boldsymbol{A} = \boldsymbol{A}_r + j\boldsymbol{A}_i \tag{A-1}$$

where $\boldsymbol{u}_r$ and $\boldsymbol{u}_i$ are two real vectors of dimension $M \times 1$ and $\boldsymbol{A}_r$ and $\boldsymbol{A}_i$ two real matrices of dimension $M \times M$. Furthermore, assume $\boldsymbol{A}$ to be Hermitian. Define

$$\boldsymbol{y} = \begin{bmatrix} \boldsymbol{u}_r \\ \boldsymbol{u}_i \end{bmatrix}, \qquad \boldsymbol{B} = \begin{bmatrix} \boldsymbol{A}_r & -\boldsymbol{A}_i \\ \boldsymbol{A}_r & \boldsymbol{A}_r \end{bmatrix}. \tag{A-2}$$

It can be shown readily that $\boldsymbol{x}^H\boldsymbol{A}\boldsymbol{x} = \boldsymbol{y}^T\boldsymbol{B}\boldsymbol{y}$ which is a real scalar, and hence

$$\int_{-\infty}^{\infty} \exp(-\boldsymbol{x}^H\boldsymbol{A}\boldsymbol{x})\, d\boldsymbol{x} = \int_{-\infty}^{\infty} \exp(-\boldsymbol{y}^T\boldsymbol{B}\boldsymbol{y})\, d\boldsymbol{y}. \tag{A-3}$$

The right-hand side of (A-3) can be evaluated exactly [16, p. 118] as

$$\int_{-\infty}^{\infty} \exp(-\boldsymbol{y}^T\boldsymbol{B}\boldsymbol{y})\, d\boldsymbol{y} = \int_{-\infty}^{\infty} \exp\left[-\frac{1}{2}\,\boldsymbol{y}^T(2\boldsymbol{B})\boldsymbol{y}\right] dy$$
$$= \frac{(2\pi)^{2M/2}}{|2\boldsymbol{B}|^{1/2}}. \tag{A-4}$$

Since [10, p. 557]

$$|2\boldsymbol{B}| = 2^{2M}|\boldsymbol{B}| = 2^{2M}|\boldsymbol{A}|^2 \tag{A-5}$$

we have from (A-3) to (A-5)

$$\int_{-\infty}^{\infty} \exp(-\boldsymbol{x}^H\boldsymbol{A}\boldsymbol{x})\, d\boldsymbol{x} = \frac{\pi^M}{|A|}. \tag{A-6}$$

APPENDIX B

Monte Carlo simulations of optimum combining with correlated branches require in general the generation of a zero-mean complex Gaussian random vector $\boldsymbol{y}$ with covariance matrix $\boldsymbol{A}$. This can be done by first generating a vector $\boldsymbol{x}$, whose elements are zero-mean unit-variance uncorrelated complex Gaussian random variables. The random vector $\boldsymbol{y}$ can then be generated from $\boldsymbol{x}$ [17, p. 251] by

$$\boldsymbol{y} = \boldsymbol{P}\boldsymbol{D}^{1/2}\boldsymbol{x} \tag{B-1}$$

where $\boldsymbol{P}$ is a matrix whose columns consist of an orthonormal set of eigenvectors of $\boldsymbol{A}$ and $\boldsymbol{D}^{1/2}$ is a diagonal matrix that consists of the square roots of the eigenvalues of $\boldsymbol{A}$. Since a covariance matrix is always Hermitian and nonnegative definite [11, p. 190], its eigenvalues are always real and nonnegative, and the existence of a real $\boldsymbol{D}^{1/2}$ is guaranteed.

ACKNOWLEDGMENT

The authors express their appreciation for the strong support and interaction provided by Bell Canada and Bell-Northern Research (now Nortel Technology).

REFERENCES

[1] R. A. Monzingo and T. W. Miller, *Introduction to Adaptive Arrays*. New York: Wiley, 1980.
[2] R. T. Compton, Jr., *Adaptive Antennas: Concepts and Performance*. Englewood Cliffs, NJ: Prentice-Hall, 1988.
[3] J. H. Winters, "Optimum combining in digital mobile radio with cochannel interference," *IEEE Trans. Veh. Technol.*, vol. VT-33, pp. 144–155, Aug. 1984.
[4] ——, "Optimum combining for indoor radio systems with multiple users," *IEEE Trans. Commun.*, vol. COM-35, pp. 1222–1230, Nov. 1987.
[5] R. G. Vaughan, "On optimum combining at the mobile," *IEEE Trans. Veh. Technol.*, vol. 37, pp. 181–188, Nov. 1988.
[6] G. V. Tsoulos, M. A. Beach, and S. C. Swales, "Performance enhancement of DSCDMA microcellular networks with adaptive antennas," in *IEEE 46th Trans. Veh. Technol. Conf.*, 1996, pp. 1086–1090.
[7] T. D. Pham and K. G. Balmain, "Proximity effects on diversity antennas," in *IEEE Conf. Universal Personal Communications*, San Diego, CA, Sept. 1994, pp. 236–241.
[8] J. Salz and J. H. Winters, "Effect of fading correlation on adaptive arrays in digital mobile radio," *IEEE Trans. Veh. Technol.*, vol. 43, pp. 1049–1057, Nov. 1994.
[9] J. R. Pierce and S. Stein, "Multiple diversity with nonindependent fading," in *Proc. IRE*, vol. 48, 1960, pp. 89–104.
[10] S. M. Kay, *Fundamentals of Statistical Signal Processing: Estimation Theory*. Englewood Cliffs, NJ: Prentice-Hall, 1993.
[11] A. Papoulis, *Probability, Random Variables, and Stochastic Processes*. New York: McGraw-Hill, 1991.
[12] W. F. Freiberger, *The International Dictionary of Applied Mathematics*. Princeton, NJ: Van Nostrand, 1960.
[13] D. H. Johnson and D. E. Dudgeon, *Array Signal Processing: Concepts and Techniques*. Englewood Cliffs, NJ: Prentice-Hall, 1993.
[14] V. M. Bogachev and I. G. Kiselev, "Optimum combining of signals in space diversity reception," *Telecommun. Radio Eng.*, vol. 34/35, pp. 83–85, Oct. 1980.
[15] P. Bello and B. D. Nelin, "Predetection diversity combining with selectively fading channels," *IRE Trans. Commun. Syst.*, vol. CS-10, p. 32, Mar. 1962.
[16] H. Cramer, *Mathematical Methods of Statistics*. Princeton, NJ: Princeton Univ. Press, 1946.
[17] A. Leon-Garcia, *Probability and Random Processes for Electrical Engineering*, 2nd ed. Reading, MA: Addison-Wesley, 1993.

Tien D. Pham (S'93–M'97) received the B.A.Sc. degree from the Engineering Academy of Denmark, Lyngby, Denmark, in 1988 and the M.A.Sc. and Ph.D. degrees from the University of Toronto, Toronto, Ont., Canada, in 1990 and 1998, respectively, all in electrical engineering.

From 1990 to 1992, he worked in the electronics industry as a Hardware Engineer. In 1996, he was a Consultant for Spar Aerospace Limited, Brampton, Canada, studying the implementation of adaptive antennas as a means to improve the quality of signals received in severe radio environments. Since 1997, he has been with the Wireless Research and Development Group, Mentor Graphics Corporation, San Jose, CA. His current research interests include adaptive antennas and microwave circuits for wireless communications.

Keith G. Balmain (S'56–M'63–SM'85–LF'87) was born in London, Ont., Canada, on August 7, 1933. He received the B.A.Sc. degree in engineering physics from the University of Toronto, Toronto, Ont., in 1957 and the M.S. and Ph.D. degrees in electrical engineering from the University of Illinois, Urbana, in 1959 and 1963, respectively.

He was an Assistant Professor of Electrical Engineering at the University of Illinois, associated primarily with the Aeronomy Laboratory, until 1966. He then joined what is now the Department of Electrical and Computer Engineering, University of Tornoto, where he is a Professor and Holder of the NSERC/Bell Canada/Nortel Industrial Research Chair in Electromagnetics. He was Chairman of the Division of Engineering Science for two and a half years until 1987, after which he chaired the University of Toronto's Research Board for a three-year term. His research has focused on antennas in plasma, broad-band antennas, radio-wave scattering from power lines and high-rise building, electrostatic charge accumulation and arc discharges on both spacecraft and human subjects, and electromagnetic compatibility. He coauthored the second edition of *Electromagnetic Waves and Radiating Systems.* He was an Associate Editor of *Radio Science* from 1978 to 1980.

Dr. Balmain was the corecipient of the IEEE Antennas and Propagation Society Best Paper of the Year Award in 1970 and the NASA Groups Achievement Award related to electrical grounding on the Space Station in 1992. His activities include membership on the IEEE Antenna Standards Committee and Chairman of the Subcommittee on Antennas in Physical Media (1968–1976), Canadian Chairman of the International Union of Radio Science Commission VI (1970–1973), member of the IEEE APS AdCom (1973–1976), and Chairman of the Technical Program Committee for the 1980 IEEE APS International Symposium held in Quebec City, Canada. Currently, he chairs the Organizing Committee for the 1999 URSI General Assembly to be held in Toronto.